A theoretical study of a spin polarized transport and giant magnetoresistance: The effect of the number of layers in a magnetic multilayer

Eun Sun Noh,[1] Hyuck Mo Lee,[1,a)] Seung-Cheol Lee,[2] and Sergio E. Ulloa[3]

[1]*Department of Materials Science and Engineering, KAIST, 335 Gwahangno, Yuseong-gu, Daejeon 305-701, Korea*
[2]*Computational Science Center, Korea Institute of Science and Technology, Hawolgok-dong 39-1, Seongbuk-gu, Seoul 136-791, Korea*
[3]*Department of Physics and Astronomy, Clippinger Laboratory 368B, Ohio University, Athens, Ohio 45701, USA*

This study presents a quantum-mechanical free electron model for analyzing a spin polarized transport and current-perpendicular-to-the-plane giant magnetoresistance (CPP-GMR) in a more realistic way. The CPP-GMR is evaluated by using three spin resolved conductance parameters based on the Landauer conductance formula. In a ballistic regime, a transfer-matrix method is used to calculate the spin dependent transmission probability as a function of the transverse mode. A spin dependent conduction band structure is constructed by extracting parameters of the free electron model, such as the atomic magnetic moments and the conduction electron densities, from the spin dependent layer-decomposed density of states of the Cu and Co interfacial layers in a Cu5/Co11 slab; these calculations are derived from the density functional theory. As a result, this study shows that the CPP-GMR in a $[\text{Cu(5 ML)}/\text{Co(11 ML)}]_n$ magnetic multilayer ($n=2-5$) with a 35 ML $\times$ 35 ML cross section is in the range of 60%–111%. It is qualitatively comparable to the calculation results of first principles. This study also uses transmission probability to explain the increase of spin dependent scattering and CPP-GMR as a function of the number of layers in the $[\text{Cu}/\text{Co}]_n$ magnetic multilayer. Moreover, the study confirms that modification of the free electron model by quantum-mechanical methods can be applied to calculations of a spin polarized transport and CPP-GMR in a specific material system. © *2008 American Institute of Physics*. [DOI: 10.1063/1.2905316]

I. INTRODUCTION

A magnetic multilayer composed of ferromagnetic and normal metals has aroused considerable interest because it exhibits the giant magnetoresistance (GMR) phenomenon due to the antiferromagnetic coupling between ferromagnets and spin dependent scattering at the ferromagnet-paramagnet interface.[1–4] Due to the large total resistance and large external magnetic field in changing the orientation of magnetization, a magnetic multilayer is less desirable in magnetic recording applications than an exchange-biased spin valve.[5,6] However, the magnetic multilayer has been continually the focus of attention because it gives valuable insight into the spin polarized transport properties.

A number of theories have been introduced to explain the fundamental physics of GMR in a magnetic multilayer. One of them is the free electron model, which has been adopted by many researchers.[7–14] However, the free electron model cannot reflect the full physics of a spin polarized transport in a specific material system because the model constructs a simple spin dependent conduction band by introducing appropriate empirical parameters and assumes that the transport in a magnetic multilayer is carried out by means of isotropic electrons with an isotropic effective mass.

Another frequently used methodology is the so-called realistic model.[15–24] The realistic model is advantageous in analyzing the specific physics of a spin polarized transport because the model quantitatively determines the spin dependent conduction band and the spin dependent phase space in a specific material system by reflecting *sp-d* or *d-d* hybridizations at the ferromagnet-paramagnet interface and by calculating the spin dependent Fermi surface.

Nonetheless, the realistic model has a few weak points. For example, it has been experimentally found that the GMR increases as a function of the number of layers in a magnetic multilayer. That is, the current-in-plane GMR (CIP-GMR) at the liquid-helium temperature is a few percent in an Fe/Cr/Fe trilayer prepared by a molecular beam epitaxy method.[25] However, the CIP-GMR at the same temperature is nearly 50% in an $[\text{Fe}/\text{Cr}]_n$ multilayer prepared by the same method.[1] Schep *et al.*[17] used the first principles calculation when reporting on the oscillation of spin dependent conductance and GMR with the number of layers in a $[\text{Cu}/\text{Co}]_n$ system. The thickness of the layers is believed to have exerted a quantum interference effect. Furthermore, the increase in the number of layers gives rise to an increase in the number of spin dependent potential steps.[10] If the height of a potential step is not very small, the increase in the num-

---

a)Author to whom correspondence should be addressed. Electronic mail: hmlee@kaist.ac.kr. Tel.: +82-42-869-3334. FAX: +82-42-869-3310.

ber of potential steps causes increased scattering. This enhancement of spin dependent scattering may be important for the increase in GMR as a function of the number of layers. However, the realistic model mainly uses a coherent potential approximation (CPA) to put complex equations into more tractable forms, and consequently, the model does not deal with scattering caused by the potential step. This approximation is inevitable in the first principles calculation because the magnetic multilayer has many phase spaces that contribute to conduction.

There is no doubt that the first principles calculation is the most appropriate method in quantitatively understanding the GMR phenomena. On the other hand, the free electron model is still necessary if the qualitative trend should be investigated in a large scale system within a few hours or if the spin dependent scattering caused by the potential step has no less important effect on GMR than the spin dependent phase space does. Combining the first principles calculation and free electron model may simultaneously satisfy the robustness of calculations and requirement of fast calculations, which is the major aim of this study.

There are two substantial differences between this study and the previous free electron model. First, this study determines the free electron model parameters not by introducing empirical parameters but by performing the first principles calculation. Namely, this study calculates the electronic structure for the Cu/Co slab such as atomic magnetic moments $[m(N), m(F)]$, conduction electron densities $[n_s(N), n_s(F)]$, and system Fermi energy (ε_F) through DFT. N stands for the normal metal and F is for the ferromagnetic one. The empirical parameters mainly carry bulk characteristics so that they cannot reflect *sp-d* or *d-d* hybridizations at the interface. Besides, experiments should precede calculations in determining the empirical parameters. Thus, the simple DFT calculation may supply more realistic parameters than the empirical parameters within a relatively short time. The quantum-mechanical free electron model adopted in this study, coupled seamlessly with the DFT calculations, can analyze the spin polarized transport and current-perpendicular-to-the-plane GMR (CPP-GMR) for a *specific* material system and not a *model* system.

This study also examines how spin dependent scattering caused by the potential step quantum mechanically contributes to CPP-GMR. Graphs of the transmission probability as a function of the transverse mode confirm that spin dependent scattering increases as the number of layers increases. In addition, a comparison of the increasing rates of scattering between majority spins and minority spins as a function of the number of layers reveals an increase in CPP-GMR.

II. COMPUTATIONAL DETAILS

The quantum-mechanical free electron model used in this study will now be summarized. The details of the derivation can be found elsewhere.[26] The CPP-GMR in a magnetic multilayer is evaluated in terms of the total resistance in parallel and antiparallel magnetizations. The equation of the total resistance given by Brataas *et al.*[27,28] is based on the relative angle of magnetization between ferromagnetic metals as well as various spin conductance parameters ($G_\uparrow$, $G_\downarrow$, and $G_{\uparrow\downarrow}^m$). The current polarization is based on the difference between $G_\uparrow$ and $G_\downarrow$; thus, the CPP-GMR is proportional to the difference between $G_\uparrow$ and $G_\downarrow$. The parameters $G_\uparrow$, $G_\downarrow$, and $G_{\uparrow\downarrow}^m$ are the spin conserving part of the spin resolved conductance parameters ($G_{\uparrow\uparrow}, G_{\downarrow\downarrow}, G_{\uparrow\uparrow\downarrow\downarrow}^m$) for which a zero spin flip probability is assumed.[29] The equations for $G_{\uparrow\uparrow}$, $G_{\downarrow\downarrow}$, and $G_{\uparrow\uparrow\downarrow\downarrow}^m$, which are based on the Landauer conductance formula,[30] are calculated by summing up all the spin dependent transmission probabilities ($T_{\uparrow\uparrow}^m, T_{\downarrow\downarrow}^m$) with the transverse mode. The transverse mode refers to the phase space available for the transport.

A transfer-matrix method in a ballistic regime is used to calculate the transmission probability as functions of the spin and transverse mode.[31] Furthermore, a plane wave form is used for the transfer-matrix method. Next, a single band effective mass approximation is used to calculate the electron momentum in a material layer.[32] The effective mass equation is composed of the effective mass, the cutoff energy, and the spin dependent conduction band edge. The effective mass is assumed to be the intrinsic electron mass, the cutoff energy is calculated from an infinite potential well model,[33] and the spin dependent conduction band edge is determined based on a Stoner description[34,35] and extraction of the free electron model parameters from the DFT calculation. In this study, the application of the atomic magnetic moment, the conduction electron density, and the system Fermi energy to the free electron model[36] combined with the Stoner exchange energy[34,35] consequently led to the determination of the spin dependent conduction band edge and the construction of a simple spin dependent conduction band structure.

The DFT calculation used in this study is performed with the Vienna *ab initio* simulation package code.[37,38] The interaction between ions and electrons is described by the projector-augmented wave method,[39] and the exchange-correlation functional is treated with a generalized-gradient approximation from the parametrization work of Perdew *et al.*[40]

This study simulates 16 atomic layers with a (1×1)-fcc structure in which the (001) plane is normal to the slab direction.[2,41] Calculations are then made of the electronic structures in the five slab systems of Cu1/Co15, Cu2/Co14, Cu3/Co13, Cu4/Co12, and Cu5/Co11. Figure 1 shows the schematic structure of the Cu5/Co11 slab. When a periodic boundary condition is applied to the calculation of the supercell, the calculation corresponds to an infinite number of layers in $[Cu/Co]_n$. Of the five slabs used, the Cu5/Co11 slab is comparable to the $[Cu(9 \text{ Å})/Co(19 \text{ Å})]_n$ multilayer, in which the thicknesses of the layers satisfy the experimental conditions.[1–4]

The self-consistent loop is iterated until the difference in the total energy is within the limit of 10^{-4} eV. The zero point vibration energy is neglected. A cutoff parameter of 450 eV (33.32 Ry) is used for the plane wave basis set. A total of 182 irreducible k points is generated for the bulk phase by means of a $12 \times 12 \times 12$ mesh of special grids within the Monkhorst–Pack scheme;[42] however, 21 irreducible k points are generated by the $12 \times 12 \times 2$ mesh for the Cu/Co slabs. The lattice constants for the Cu and Co (ferromagnetic state)
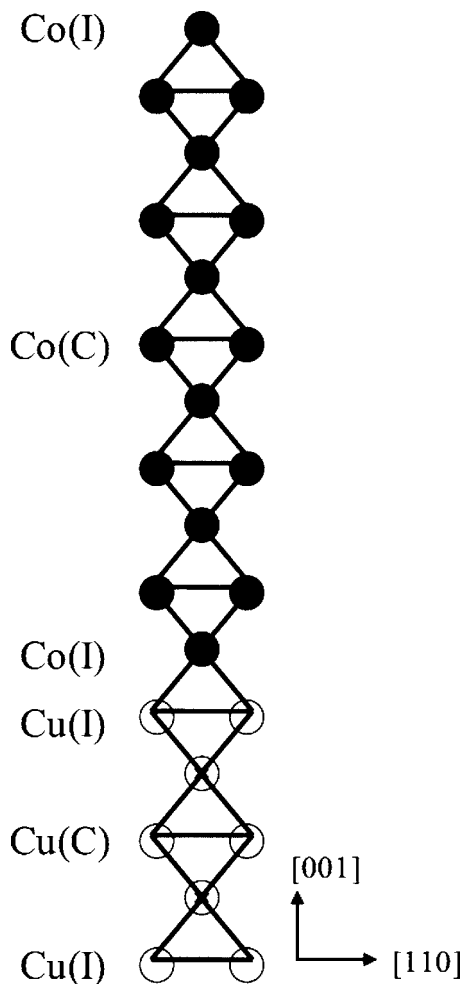
FIG. 1. Schematic structure of the Cu5/Co11 slab with a (1×1)-fcc structure where the (001) plane is normal to the slab direction. The open circles denote Cu atoms and the filled circles denote Co atoms. The parameter I stands for the interface and C is the center.

fcc bulks are estimated to be 3.646 and 3.528 Å, respectively. The ionic relaxation of the Cu/Co slab is not considered, and thus, the values of the lattice constant (3.528 Å) and Wigner–Seitz radius (1.25 Å) for the Co fcc bulk are used for the Cu/Co slab. This condition is reasonable for evaluation of the electronic structure in the Cu/Co slab because Cu and Co are both transition metals and their lattice constants are similar.

III. RESULTS

A. Electronic structure of the Cu5/Co11 multilayer

Figure 2 shows the spin dependent LDOS of the 4s, 4p, and 3d bands in the Cu fcc bulk, the Co fcc bulk, and the Cu5/Co11 slab. As demonstrated in Figs. 2(a) and 2(b), the d-like bands of Cu are fully occupied and located at about 2 eV below the Fermi level. Only the s-like bands of Cu cross the Fermi level. The LDOS of the Cu bulk does not show spin polarization; however, in the case of the Cu interfacial layer denoted by Cu(I), the LDOS of the minority spin d band at the Fermi level is larger than that of the majority spin. As shown in Figs. 2(c) and 2(d), the LDOS of the Co interfacial layer is different from that of the bulk. Hence, Fig.
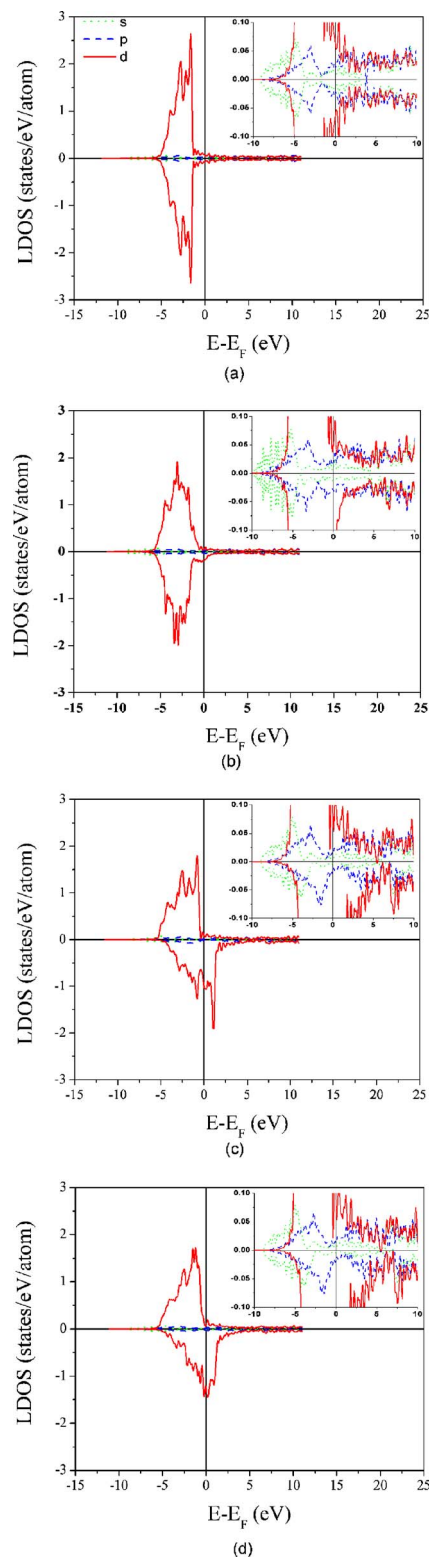

FIG. 2. (Color online) Spin dependent LDOS of 4s, 4p, and 3d bands in a Cu fcc bulk, a Co fcc bulk, and a Cu5/Co11 slab: (a) the Cu fcc bulk, (b) the Cu(I) layer, (c) the Co fcc bulk, and (d) the Co(I) layer. The inset shows an enlarged one near the zero value of LDOS.

2 confirms that the free electron model, depending on the empirical parameters, is not appropriate in describing the interfacial scattering in this system.

Table I shows the spin resolved charges of the 4s, 4p, and 3d bands in the Cu fcc bulk, the Co fcc bulk, and the

TABLE I. Spin-resolved charge of the 4s, 4p, and 3d bands, the layer-decomposed total electron density (Q), and the layer-decomposed atomic magnetic moment (M) in the Cu fcc bulk, the Co fcc bulk, and the Cu5/Co11 slab. The parameter I stands for the interface and C is the center.

Atom	Spins	4s	4p	3d	Q/M
Cu bulk	↑	0.200 18	0.163 10	4.569 11	9.864 94
	↓	0.200 17	0.163 10	4.569 28	−0.006 97
Cu bulk	↑	0.188 21	0.173 34	4.429 00	7.869 89
	↓	0.195 48	0.210 52	2.673 34	1.711 21
Cu(I)	↑	0.217 04	0.196 43	4.593 39	9.988 76
	↓	0.255 90	0.214 88	4.541 12	0.024 96
Co(I)	↑	0.185 27	0.173 31	4.369 88	7.842 68
	↓	0.187 03	0.192 36	2.734 83	1.614 24
Cu(C)	↑	0.215 68	0.195 91	4.577 97	9.979 87
	↓	0.216 49	0.196 99	4.576 83	0.000 75
Co(C)	↑	0.187 35	0.173 80	4.416 61	7.856 34
	↓	0.195 27	0.209 70	2.673 61	1.699 18

TABLE II. Spin dependent LDDS at the Fermi level of the 4s, 4p, and 3d bands and the layer-decomposed conduction electron density (n_s) in the Cu fcc bulk, the Co fcc bulk, and the Cu5/Co11 slab. The parameter I stands for the interface and C is the center.

Atoms	Spins	4s	4p	3d	n_s
Cu bulk	↑	0.013 48	0.025 46	0.066 32	⋯
	↓	0.013 48	0.025 45	0.066 29	0.210 48
Co bulk	↑	0.009 75	0.013 92	0.089 08	⋯
	↓	0.003 50	0.015 62	1.000 75	0.131 87
Cu(I)	↑	0.009 61	0.019 30	0.049 43	⋯
	↓	0.012 77	0.029 61	0.187 17	0.307 89
Co(I)	↑	0.006 13	0.017 71	0.082 81	⋯
	↓	0.005 81	0.025 79	1.264 67	0.138 25
Cu(C)	↑	0.013 20	0.028 80	0.055 24	⋯
	↓	0.011 42	0.022 46	0.055 58	0.186 70
Co(C)	↑	0.004 64	0.014 39	0.046 11	⋯
	↓	0.002 74	0.021 38	0.956 73	0.089 26

Cu5/Co11 slab. The electron density is determined by integrating the LDOS in Fig. 2 from the band edge to the Fermi level. The layer-decomposed total electron density and the layer-decomposed atomic magnetic moment are also shown. The total electron density is calculated by summing up all the electron densities with the band and with the spin state. The atomic magnetic moment is determined as the difference of the total electron densities between the majority and minority spins. According to Table I, the total electron density for the Cu interfacial layer (9.99) is about 0.13 larger than that of the Cu bulk (9.86), whereas the total electron density for the Co interfacial layer (7.84) is about 0.03 smaller than that of the Co bulk (7.87). Vlaic *et al.*[43] showed that electrons are transferred from M atoms to Cu atoms at the M/Cu (M=Fe or Co) interface due to the relative position of the Fermi levels. Although the pseudopotential approximation cannot give the exact position of the Fermi level, the Fermi energies are 3.57 eV for the Cu bulk and 5.40 eV for the Co bulk. Furthermore, the experimental work functions have been reported to be 4.65 eV for the Cu bulk and 5.0 eV for the Co bulk.[44] These work functions can explain the net charge transfer from Co atoms to Cu atoms.

Table I also shows that for the Cu interfacial layer, the electron densities of the majority and minority spin d bands (4.59, 4.54) are about 0.02 bigger and about 0.03 smaller than the corresponding values of the Cu bulk (4.57). For the Co interfacial layer, the electron densities of the majority and minority spin d bands (4.37, 2.73) are about 0.06 smaller and about 0.06 bigger than the corresponding values of the Co bulk (4.43, 2.67). A reverse charge transfer of the minority spin d band in the interfacial layer causes a difference in the atomic magnetic moments between the bulk and the interfacial layer. The magnetization in this case is induced in the Cu interfacial layer, and the atomic magnetic moment is reduced in the Co interfacial layer. As shown in Table I, the atomic magnetic moment for the Cu interfacial layer is 0.025, though the Cu in the bulk and that in the centered layer do not have an atomic magnetic moment. The atomic magnetic moment for the Co interfacial layer is 1.614, though the atomic magnetic moments are 1.71 for the Co bulk and 1.70 for the Co centered layer.

By using the full-potential linearized augmented plane wave method, Li *et al.*[45] and Klautau and Frota-Pessoa[46] reported that the atomic magnetic moment of the Co centered layer in the fcc (001) Co film is 1.65. Pentcheva and Scheffler[47] used the same method and reported that the atomic magnetic moment of a Co fcc bulk is 1.52. It therefore seems that the projector-augmented wave generalized-gradient approximation method slightly overestimates the atomic magnetic moment.

Table II shows the spin dependent LDOS at the Fermi level of the 4s, 4p, and 3d bands in the Cu fcc bulk, the Co fcc bulk, and the Cu5/Co11 slab. The layer-decomposed conduction electron density is also listed. As shown in Figs. 2(a) and 2(b), all the bands of Cu at the Fermi level are close to the s-like band. However, Figs. 2(c) and 2(d) show that most bands of Co at the Fermi level are the s-like band but the minority spin d band is localized. This study determines the conduction electron density in accordance with Stearns'[48] model. The procedure is as follows. All the bands of Cu are assumed to have an isotropic effective mass as the intrinsic electron mass, and the conduction electron density of Cu is consequently derived by summing up all the LDOS values at the Fermi level with the band and the spin state. However, the effective mass of the minority spin d band of the Co is assumed to be so large that this band does not particularly contribute to conduction in a magnetic multilayer. The other bands of Co are also assumed to have an isotropic effective mass as the intrinsic electron mass. Consequently, this study calculates the conduction electron density of Co by summing up the LDOS values at the Fermi level for the s and p bands and the majority spin d band.

To construct the spin dependent conduction band structure by using a free electron model, this study uses the elec-
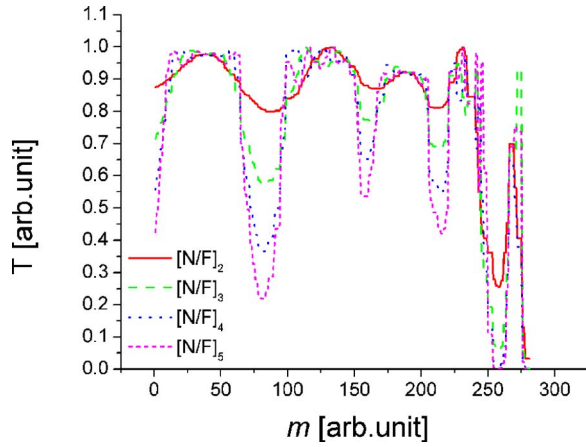
FIG. 3. (Color online) Spin independent transmission probability as a function of the transverse mode in the $[N(5\ \text{ML})/F(11\ \text{ML})]_n$ magnetic multilayer with the zero Stoner exchange parameter and a 35×35 ML^2 cross section. The size of a monolayer is determined based on the lattice constant of the Cu5/Co11 slab (3.528 Å) so that the thicknesses of the ferromagnetic and normal metals are almost the same as those of the Cu5/Co11 slab.

tronic structures for the Cu and Co interfacial layers shown in Tables I and II because the interfacial electronic structure mainly affects the spin polarized transport and GMR.[49,50] Table I shows that the values of $m(N)$ and $m(F)$ in the $[N/F]_n$ magnetic multilayer are 0.025 and 1.614, respectively, while Table II shows that the values of $n_s(N)$ and $n_s(F)$ are 0.31 and 0.14. The value of ε_F in the $[N/F]_n$ magnetic multilayer is 5.11 eV, which is the Fermi energy in the Cu5/Co11 slab. The Stoner exchange parameter in the $[N/F]_n$ magnetic multilayer is 0.99 eV, which is the Stoner parameter for the Co bulk.[34,35] As a result, the values of $n_s^\uparrow(N)$ and $n_s^\downarrow(N)$ as determined by $n_s(N)$ and $m(N)$ are larger than the values of $n_s^\uparrow(F)$ and $n_s^\downarrow(F)$ as determined by $n_s(F)$ and $m(F)$. A normal metallic layer consequently becomes a quantum well with a magnetic barrier in the $[N/F]_n$ magnetic multilayer.

B. Transmission probability and CPP-GMR in the $[N/F]_n$ multilayer

Figure 3 shows the spin independent transmission probability as a function of the transverse mode in the $[N(5\ \text{ML})/F(11\ \text{ML})]_n$ (ML stands for monolayer) multilayer with the zero Stoner exchange parameter. All transmission probabilities fluctuate over all the transverse modes with four dips mainly due to the resonant state at the specific transverse modes. In other words, the electron momentum decreases as a function of the transverse mode,[32,33] and consequently, the transmission probability generally decreases with the transverse mode. However, if the quantum well state energies that depend on the thickness of a normal metallic layer are identical to the cutoff energies that depend on the cross sectional size, resonance is formed and the transmission probabilities at the resonant transverse modes become[51] 1.0.

Figure 3 also shows that spin independent coherent scattering increases as a function of the number of layers. That is, an increase in the number of layers gives rise to an in-

crease in the number of potential steps. As a result, the depth of the four dips and the fluctuation amplitude increase as a function of the number of layers. The increased scattering is notable at the four dips because the number of transverse modes, the position of the four dips, and the fluctuation frequency are identical irrespective of the number of layers.

Figure 4 shows the spin dependent transmission probability as a function of the transverse mode in the $[N(5\ \text{ML})/F(11\ \text{ML})]_n$ magnetic multilayer. The number of transverse modes for the majority spins is larger than the zero Stoner exchange parameter in Fig. 3, and the opposite is true for the minority spins. In addition, the value of $T_{\uparrow\uparrow}^m$ is almost 1.0 at the low transverse mode with one weak dip and the value of $T_{\uparrow\uparrow}^m$ fluctuates at the high transverse mode with four dips. However, the value of $T_{\downarrow\downarrow}^m$ fluctuates over all the transverse modes with two strong dips. The differences in the number of transverse modes and scatterings between the majority and minority spins are the result of the difference in the heights of the potential steps between the majority and minority spins. That is, because $m(F)$ is much larger than $m(N)$, the difference between $n_s^\uparrow(N)$ and $n_s^\uparrow(F)$ is smaller than the difference between $n_s(N)$ and $n_s(F)$, and the difference between $n_s^\downarrow(N)$ and $n_s^\downarrow(F)$ is larger than the difference between $n_s(N)$ and $n_s(F)$. Consequently, the potential step height for the majority spins is smaller than the zero Stoner exchange parameter in Fig. 3, whereas that of the minority spins is larger. This difference between the majority and minority spins has a strong effect on the current polarization and, in turn, on the CPP-GMR.

Figure 4 also shows that the spin dependent scattering increases as a function of the number of layers. The increase in the spin dependent scattering is basically the same as that in the zero Stoner exchange parameter in Fig. 3. In other words, the depth of the dips and the fluctuation amplitude increase with the number of layers, whereas the number of transverse modes, the position of the dips, and the fluctuation frequency are identical irrespective of the number of layers.

It is difficult to compare the increasing rate of scatterings between the majority and minority spins from Fig. 4 alone. Nevertheless, this comparison is important because, for both the majority and minority spins, the number of transverse modes is identical irrespective of the number of layers, and thus, the difference in the increasing rates of scatterings is the main reason why the CPP-GMR changes with the number of layers. The decrease of $T_{\uparrow\uparrow}^m$ with the number of layers mainly occurs at the high transverse mode and the decrease of $T_{\downarrow\downarrow}^m$ occurs over all the transverse modes. Thus, by inference, the increasing rate in scattering is larger for the minority spins than for the majority spins.

Table III shows the spin conductance parameters and CPP-GMR in the $[N(5\ \text{ML})/F(11\ \text{ML})]_n$ magnetic multilayer. The spin conductance parameters decrease as a function of the number of layers because, as shown in Fig. 4, the average transmission probability decreases as the number of layers decreases. Moreover, the difference between $G_\uparrow$ and $G_\downarrow$ and the CPP-GMR increases as a function of the number of layers. As mentioned, the increasing rate of scattering is highly likely to be larger for the minority spin than for the majority spin.
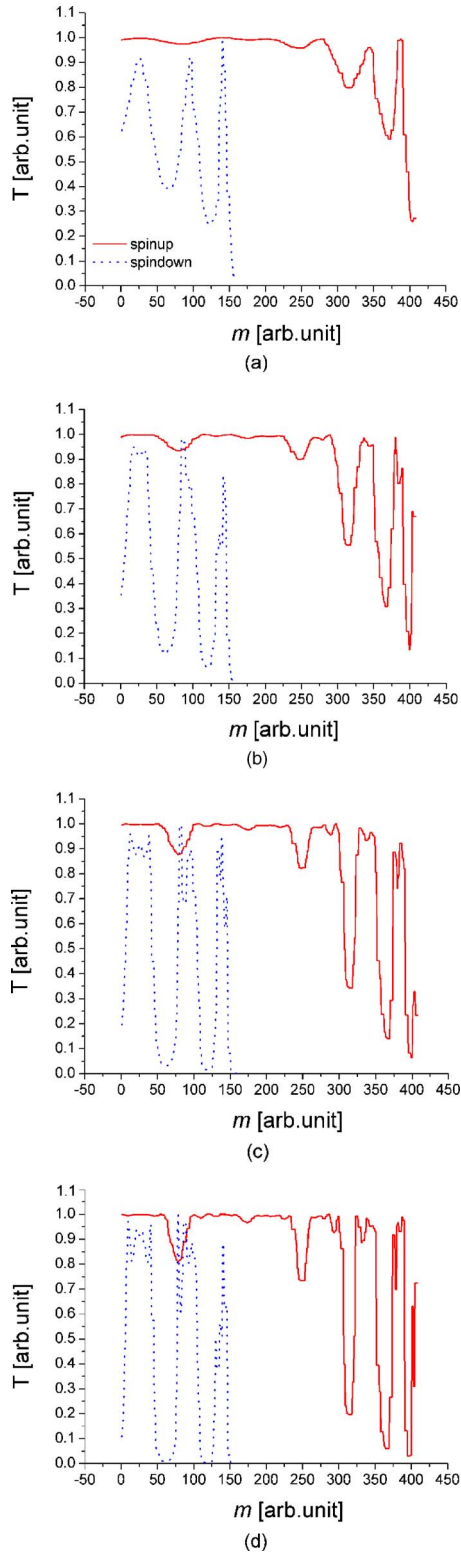
FIG. 4. (Color online) Spin dependent transmission probability as a function of the transverse mode in (a) $[N(5\ \mathrm{ML})/F(11\ \mathrm{ML})]_2$, (b) $[N(5\ \mathrm{ML})/F(11\ \mathrm{ML})]_3$, (c) $[N(5\ \mathrm{ML})/F(11\ \mathrm{ML})]_4$, and (d) $[N(5\ \mathrm{ML})/F(11\ \mathrm{ML})]_5$ magnetic multilayers with a $35 \times 35\ \mathrm{ML}^2$ cross section.

TABLE III. Spin conductance parameters (in units of $10^3\ \Omega^{-1}$) and CPP-GMR (in percentage) in the $[N(5\ \mathrm{ML})/F(11\ \mathrm{ML})]_n$ magnetic multilayer with a $35 \times 35\ \mathrm{ML}^2$ cross section.

	$[N/F]_2$	$[N/F]_3$	$[N/F]_4$	$[N/F]_5$
$G_\uparrow$	14.527	14.089	13.703	13.635
$G_\downarrow$	3.489	2.914	2.449	2.321
$G_{\uparrow\downarrow}^m$	4.610	4.026	3.744	3.600
CPP-GMR (%)	60.096	76.044	94.352	111.121

of using DFT calculations to extract the free electron model parameters from the electronic structures of the Cu and Co interfacial layers, which has already been explained, was performed to reflect *sp-d* or *d-d* hybridizations at the Cu/Co interface of a free electron model. As a result, the CPP-GMR in the $[\mathrm{Cu}(5\ \mathrm{ML})/\mathrm{Co}(11\ \mathrm{ML})]_n$ magnetic multilayer ($n = 2 - 5$) is calculated in the range of 60%–111%. By using only the first principles calculation, Schep *et al.*[17] reported that the CPP-GMR in the $[\mathrm{Cu}(1\ \mathrm{ML})/\mathrm{Co}(1\ \mathrm{ML})]_n$ magnetic multilayer ($n = 1 - 8$) is in the range of 60%–120%. Moreover, this study confirmed that CPP-GMR increases as a function of the number of layers in the $[\mathrm{Cu}/\mathrm{Co}]_n$ magnetic multilayer. By combining the free electron model and the DFT calculation, this work showed a qualitative behavior of the spin polarized transport and CPP-GMR in the $[\mathrm{Cu}/\mathrm{Co}]_n$ magnetic multilayer.

There are certain limitations in the application of the previous free electron model to a specific material system. It is difficult to experimentally investigate the electronic structure of the interfacial layer in a magnetic multilayer. Thus, the parameters of the free electron model are usually extracted from the values of a specific bulk material. The quantum-mechanical free electron model parametrized by DFT calculations offers more realistic parameters than the previous free electron model.

The most desirable way of analyzing the spin polarized transport in a specific material system is to calculate the spin dependent Fermi surface by first principles because it enables a quantitative investigation of the spin polarized transport. For some cases, a quantitative analysis is really important. However, from the point of practical applications, a qualitative study may be sufficient. Furthermore, because of the time-consuming nature of calculating the Fermi surface, this kind of calculation is mainly used in small scale systems and it generally gives rise to a quantum interference or quantum size effect. A quantum-mechanical free electron model is more advantageous than the first principles calculation because it is faster and can deal with larger systems.

To hasten the calculation time, this study did not consider the ionic relaxation of the Cu/Co slab and it used the pseudopotential instead of the full potential. Nevertheless, the calculations yielded reliable qualitative information for the $[\mathrm{Cu}/\mathrm{Co}]_n$ magnetic multilayer because Cu and Co are both metallic materials and their lattice constants are similar. In fact, the conditions for the DFT calculations are system dependent. For example, Kim *et al.*[52] reported that ionic relaxation is important in an Al/Co system due to the difference between the structural and physical properties of Al and Co.

IV. DISCUSSION

The electronic structure in the Cu5/Co11 slab, which was attained by DFT calculations, exhibits a difference between the bulk and interfacial layer. Furthermore, the process

This study obtained the spin dependent transmission probability as a function of the transverse mode, and it emphasized the spin dependence of the potential step and the electron wave properties. This study also explained how the number of potential steps affects the electron wave properties. An increase of GMR with the number of potential steps has already been demonstrated by the previous free electron model, though it mainly dealt with GMR in a semiclassical approach. In that approach, it was difficult to give a specific explanation for the fundamental quantum physics for the spin dependent scattering. On the other hand, due to the enormous amount of calculations, the first principles calculation usually neglects the transmission probability and focuses on the accurate calculation of the spin dependent electronic structure. For example, Butler *et al.*[18–20] and Kudrnovsky and co-workefrs[23,24] used the CPA with the layer Korringa–Kohn–Rostoker (KKR) method or with the tight-binding linear muffin-tin orbital (TB-LMTO) approach to describe the spin polarized transport in the $[Cu/Co]_n$ magnetic multilayer. The CPA equalizes the transmission probabilities with the quantum states by replacing the individual transfer matrices with the coherent transfer matrices. Furthermore, Schep *et al.*[17] assumed all the transmission probabilities with the transverse modes to be 1.0 by using the Sharvin conductance formula and calculated the CPP-GMR in the $[Cu/Co]_n$ magnetic multilayer by calculating the spin dependent Fermi surface in terms of the LMTO method. Besides, Zahn *et al.*[21,22] dealt with the spin dependent scattering semiclassically by using the empirical parameter such as the spin anisotropy ratio β and showed that the CPP-GMR is in the range of 200%–300% by using the TB-KKR method. This study puts emphasis on analyzing the transmission probability in relation to the height and number of potential steps.

Even if all the potentials in a system are simplified by a free electron model, a long time is needed to calculate all the transmission probabilities for the large number of phase spaces that the first principles calculation deals with. Thus, in this study, the magnetic multilayer was examined on a small scale such as a cross section of 35×35 ML.[2] This condition is feasible because the quantum-mechanical free electron model used in this study has shown that the geometrical size of the cross section does not affect the qualitative trend of the spin polarized transport and CPP-GMR.

This study presents a quantum-mechanical and visible understanding of the spin dependent scattering in relation to the number of potential steps. In conclusion, when this model is used in conjunction with the DFT calculation and the transfer-matrix method, it can be the most appropriate analytical tool for dealing with specific cases such as the effect of the number of layers on spin polarized transport. Besides, this model can include the effect of the nonideal interfaces such as defects or surface segregation on the spin polarized transport with the help of DFT calculations.

V. SUMMARY

This study presents a combination of a quantum-mechanical free electron model with the DFT calculation and a transfer-matrix method for analyzing spin polarized transport and CPP-GMR in a specific material system. The capability of the quantum-mechanical free electron model is verified by the value of the CPP-GMR, which is comparable to the results of the first principles calculation in the $[Cu/Co]_n$ magnetic multilayer, and by the fact that spin dependent scattering and CPP-GMR increase as a function of the number of layers. With a correction to the free electron model and the transfer-matrix method and the performance of an exact DFT calculation, the model may be used to analyze the spin polarized transport in a magnetic multilayer composed of a semiconductor or an insulator.

ACKNOWLEDGMENTS

[1] M. N. Baibich, J. M. Broto, A. Fert, F. N. Van Dau, F. Petroff, P. Eitenne, G. Creuzet, A. Friederich, and J. Chazelas, Phys. Rev. Lett. **61**, 2472 (1988).
[2] S. S. P. Parkin, R. Bhadra, and K. P. Roche, Phys. Rev. Lett. **66**, 2152 (1991).
[3] D. H. Mosca, F. Petroff, A. Fert, P. A. Schroeder, W. P. Pratt, and R. Laloee, J. Magn. Magn. Mater. **94**, L1 (1991).
[4] R. Nakatani, T. Dei, T. Kobayashi, and Y. Sugita, IEEE Trans. Magn. **28**, 2668 (1992).
[5] B. Dieny, V. S. Speriosu, S. S. P. Parkin, B. A. Gurney, D. R. Wilhoit, and D. Mauri, Phys. Rev. B **43**, 1297 (1991).
[6] J. J. Qiu, K. B. Li, P. Luo, Y. K. Zheng, and Y. H. Wu, J. Magn. Magn. Mater. **272**, 1447 (2004).
[7] R. Q. Hood and L. M. Falicov, Phys. Rev. B **46**, 8287 (1992).
[8] R. E. Camley and J. Barnas, Phys. Rev. Lett. **63**, 664 (1989).
[9] J. Barnas, A. Fuss, R. E. Camley, P. Grunberg, and W. Zinn, Phys. Rev. B **42**, 8110 (1990).
[10] G. E. W. Bauer, Phys. Rev. Lett. **69**, 1676 (1992).
[11] T. Valet and A. Fert, Phys. Rev. B **48**, 7099 (1993).
[12] S. Zhang and P. M. Levy, J. Appl. Phys. **69**, 4786 (1991).
[13] M. Johnson, Phys. Rev. Lett. **67**, 3594 (1991).
[14] A. Vedyayev, C. Cowache, N. Ryzhanova, and B. Dieny, J. Phys.: Condens. Matter **5**, 8289 (1993).
[15] Y. Asano, A. Oguri, and S. Maekawa, Phys. Rev. B **48**, 6192 (1993).
[16] H. Itoh, J. Inoue, and S. Maekawa, Phys. Rev. B **51**, 342 (1995).
[17] K. M. Schep, P. J. Kelly, and G. E. W. Bauer, Phys. Rev. Lett. **74**, 586 (1995).
[18] W. H. Butler, X. G. Zhang, D. M. C. Nicholson, and J. M. MacLaren, J. Appl. Phys. **76**, 6808 (1994).
[19] W. H. Butler, X. G. Zhang, D. M. C. Nicholson, and J. M. MacLaren, Phys. Rev. B **52**, 13399 (1995).
[20] W. H. Butler, X. G. Zhang, D. M. C. Nicholson, T. C. Schulthess, and J. M. MacLaren, Phys. Rev. Lett. **76**, 3216 (1996).
[21] P. Zahn, I. Mertig, M. Richter, and H. Eschrig, Phys. Rev. Lett. **75**, 2996 (1995).
[22] P. Zahn, J. Binder, I. Mertig, R. Zeller, and P. H. Dederichs, Phys. Rev. Lett. **80**, 4309 (1998).
[23] J. Kudrnovsky, V. Drchal, I. Turek, P. H. Dederichs, P. Weinberger, and P. Bruno, J. Magn. Magn. Mater. **240**, 177 (2002).
[24] O. Bengone, O. Eriksson, S. Mirbt, I. Turek, J. Kudrnovsky, and V. Drchal, Phys. Rev. B **69**, 092406 (2004).
[25] A. Chaiken, T. M. Tritt, D. J. Gillespie, J. J. Krebs, P. Lubitz, M. Z. Harford, and G. A. Prinz, J. Appl. Phys. **69**, 4798 (1991).
[26] E. S. Noh, H. M. Lee, and S. E. Ulloa, J. Korean Phys. Soc. **48**, 451 (2006).
[27] A. Brataas, Y. V. Nazarov, and G. E. W. Bauer, Eur. Phys. J. B **22**, 99 (2001).
[28] A. Brataas, Y. V. Nazarov, and G. E. W. Bauer, Phys. Rev. Lett. **84**, 2481 (2000).

[29]Y. Li and C. R. Chang, J. Magn. Magn. Mater. **277**, 344 (2004).

[30]S. Maekawa and T. Shinjo, *Spin Dependent Transport in Magnetic Nanostructures* (Taylor & Francis, New York, 2002), Chap. 2.

[31]D. Csontos, Ph.D. thesis, Lund University, 2002.

[32]S. Datta, *Electronic Transport in Mesoscopic Systems* (Cambridge University Press, Cambridge, 1995), Chap. 1.

[33]R. Eisberg and R. Resnick, *Quantum Physics of Atoms, Molecules, Solids, Nuclei and Particles* (Wiley, New York, 1985).

[34]O. Gunnarsson, J. Appl. Phys. **49**, 1399 (1978).

[35]Z. V. Sljivancanin and F. R. Vukajlovic, J. Phys.: Condens. Matter **10**, 8679 (1998).

[36]C. Kittel, *Introduction to Solid State Physics* (Wiley, New York, 1996), Chap. 6.

[37]G. Kresse and J. Hafner, Phys. Rev. B **47**, 558 (1993).

[38]G. Kresse and J. Furthmuller, Vienna *ab initio* simulation package, University of Wien, Vienna, 2001).

[39]P. E. Blochl, Phys. Rev. B **50**, 17953 (1994).

[40]J. P. Perdew, K. Burke, and M. Ernzerhof, Phys. Rev. Lett. **77**, 3865 (1996).

[41]P. Alippi, P. M. Marcus, and M. Scheffler, Phys. Rev. Lett. **78**, 3892 (1997).

[42]H. J. Monkhorst and J. D. Pack, Phys. Rev. B **13**, 5188 (1976).

[43]P. Vlaic, M. Alouani, H. Dreyss, O. Bengone, and I. Turek, J. Appl. Phys. **96**, 4352 (2004).

[44]H. B. Michaelson, J. Appl. Phys. **48**, 4729 (1977).

[45]C. Li, A. J. Freeman, and C. L. Fu, J. Magn. Magn. Mater. **75**, 53 (1988).

[46]A. B. Klautau and S. Frota-Pessoa, Surf. Sci. **497**, 385 (2002).

[47]R. Pentcheva and M. Scheffler, Phys. Rev. B **61**, 2211 (2000).

[48]M. B. Stearns, J. Magn. Magn. Mater. **5**, 167 (1977).

[49]P. M. Levy, S. Zhang, and A. Fert, Phys. Rev. Lett. **65**, 1643 (1990).

[50]A. Barthelemy, A. Fert, M. N. Baibich, S. Hadjoudj, F. Petroff, P. Etienne, R. Cabanel, S. Lequien, F. N. Van Dau, and G. Creuzet, J. Appl. Phys. **67**, 5908 (1990).

[51]M. J. Kelly, *Low Dimensional Semiconductors Materials, Physics, Technology, Devices* (Oxford University Press, London, 2000), Chap. 4.

[52]S. P. Kim, J. Appl. Phys. **93**, 8564 (2003).